Selective photoreduction of carbon dioxide to formic acid using $Cs_3Bi_2Cl_9$-Ir/IrO_X hybrid materials

*Govardhan Pandurangappa, Alamelu Kaliyaperumal, Raghuram Chetty, * and Aravind Kumar Chandiran**

Department of Chemical Engineering, Indian Institute of Technology Madras, Chennai,Tamil Nadu 600036, India.

*raghuc@iitm.ac.in, aravindkumar@iitm.ac.in

Electronic Supplementary Information

Table S1. Iridium content analysis of catalyst samples by ICP-OES.

S. No	Sample	g	Wavelength (nm)	Dilution Factor
1	$Cs_3Bi_2Cl_9$	0.0156	Bi-223.061	10
2	$Cs_3Bi_2Cl_9$-Ir/IrO_X	0.0157	Bi-223.061	10
		0.0157	Ir-205.222	1

Table.S2. Fitting parameters for time resolved PL studies using a tri-exponential function.

Sample	τ_1 (ns)	A_1	τ_2(ns)	A_2	τ_3(ns)	A_3
$Cs_3Bi_2Cl_9$	3.85	33.84	12.36	31.04	0.52	35.12
$Cs_3Bi_2Cl_9$-Ir/IrO_X	4.55	28.05	13.17	19.06	0.46	52.89

Where A_1, A_2, and A_3 are relative amplitudes.

Table.S3. EDAX analysis of $Cs_3Bi_2Cl_9$.

Element	Weight (%)	Atomic (%)
Cl K	26.82	62.75
Cs L	36.09	22.52
Bi M	37.09	14.72
Totals		100.00

Table.S4. EDAX analysis of $Cs_3Bi_2Cl_9$-Ir/IrO_X.

Element	Weight (%)	Atomic (%)
Cl K	23.61	58.87
Cs L	35.74	23.76
Ir M	4.86	2.24
Bi M	35.79	15.14
Totals		100.00

Table.S5. A comparison of data with other materials which belongs to same class.

Catalyst	Light source	Reaction mode	Product (μmol g^{-1} h^{-1})	Ref.
$Cs_3Bi_2Cl_9$ $Cs_3Bi_2Br_9$ $Cs_3Bi_2I_9$	300W Xe arc lamp	Gas-solid (CO_2 + H_2O)	CO-16.6 CO-26.9 CO-1.1	[1]
$Cs_3Bi_2(Cl_{0.5}Br_{0.5})_9$ $Cs_3Bi_2(Br_{0.5}I_{0.5})_9$ $Cs_3Bi_2I_9$	300 W Xe arc lamp λ > 420 nm	Gas-solid (CO_2 + H_2O)	CO-16 CO-18 CO-3.6	[2]
$Cs_3Bi_2I_9$ $Rb_3Bi_2I_9$ $(CH_3NH_3)_3Bi_2I_9$	32 W UV-B (305 nm)	Gas-solid (CO_2 + H_2O)	CO-7.7, CH_4-1.4 CO-1.8, CH_4-1.7 CO-0.7, CH_4-0.9	[3]
$Cs_3Bi_2Br_9$ (CBB) 3CBB/Bi-MOF 3CBB: Bi-MOF Bi-MOF	300 W Xe lamp	Gas-solid (CO_2 + H_2O)	CO-150, CH_4-11.5 CO-572.2, CH_4-32.5 CO-230, CH_4-8.0 CO-130, CH_4-7.0	[4]
$Cs_3Bi_2I_9$ $Cs_3Bi_2I_9$/ Bi_2WO_6 $Cs_3Bi_2I_9$:Bi_2WO_6 Bi_2WO_6	300 W Xe arc lamp λ > 400 nm	Gas-solid (CO_2 + H_2O)	CO-1.8 CO-7.3 CO-2.5 CO-0.2	[5]
$Cs_2Bi_2Cl_9$	5 W UV Led	Acetonitrile + H_2O (99:1 vol%)	HCOOH-115.6 CO-53.8 CH_4-6.7	This work
$Cs_2Bi_2Cl_9$-Ir/IrO_X	5 W UV Led	Acetonitrile + H_2O (99:1 vol%)	HCOOH -168.2 CO-38 CH_4-4.5	This work

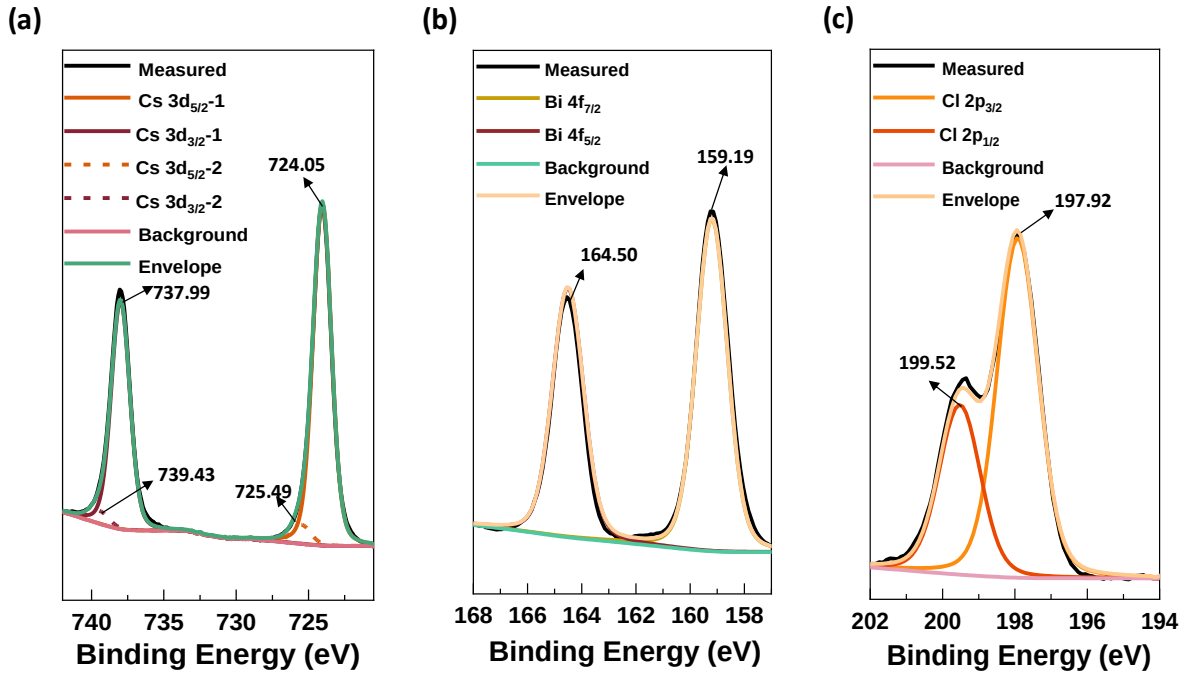

Figure S1. XPS analysis of $Cs_3Bi_2Cl_9$ before CO_2 photoreduction: (a) Cs *3d* (b) Bi *4f* (c) Cl *2p*.

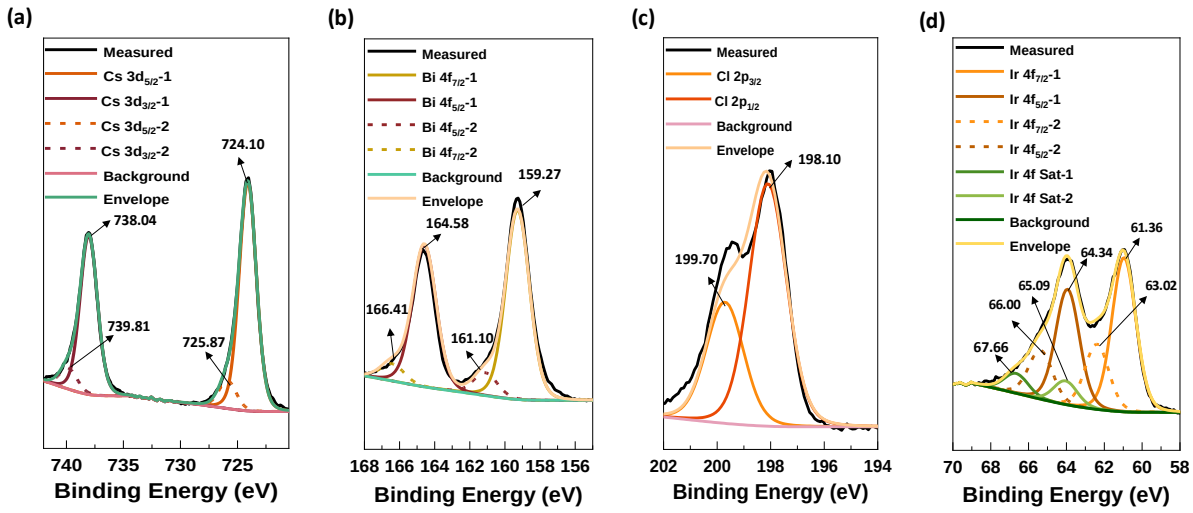

Figure S2. XPS analysis of $Cs_3Bi_2Cl_9$-Ir/IrO_X before CO_2 photoreduction: (a) Cs 3d (b) Bi 4f (c) Cl 2p (d) Ir 4f.

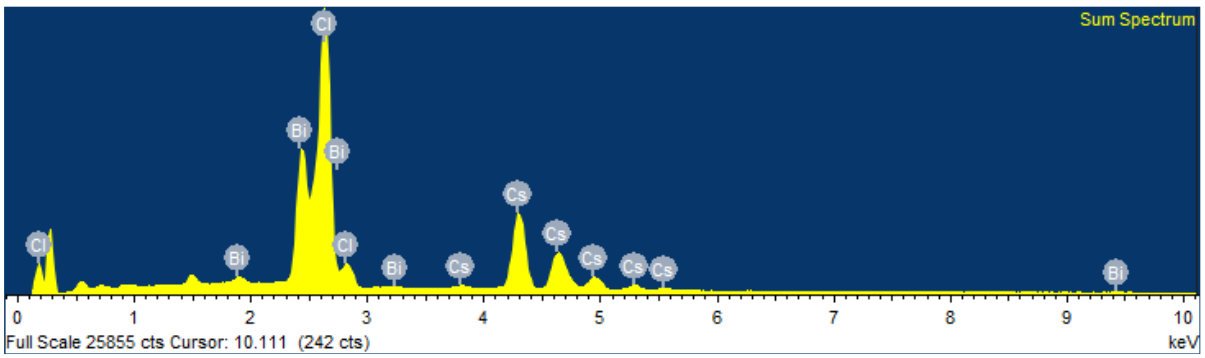

Figure.S3. EDAX spectra of $Cs_3Bi_2Cl_9$.

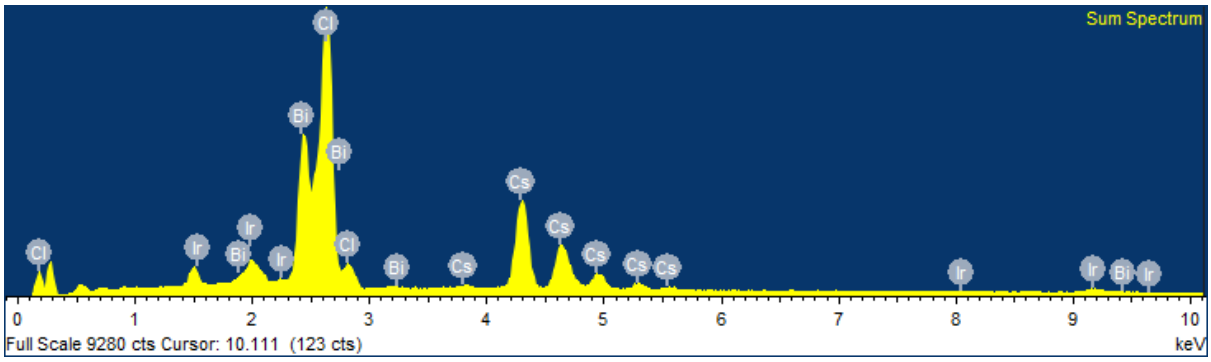

Figure.S4. EDAX spectra of $Cs_3Bi_2Cl_9$-Ir/IrO_X.

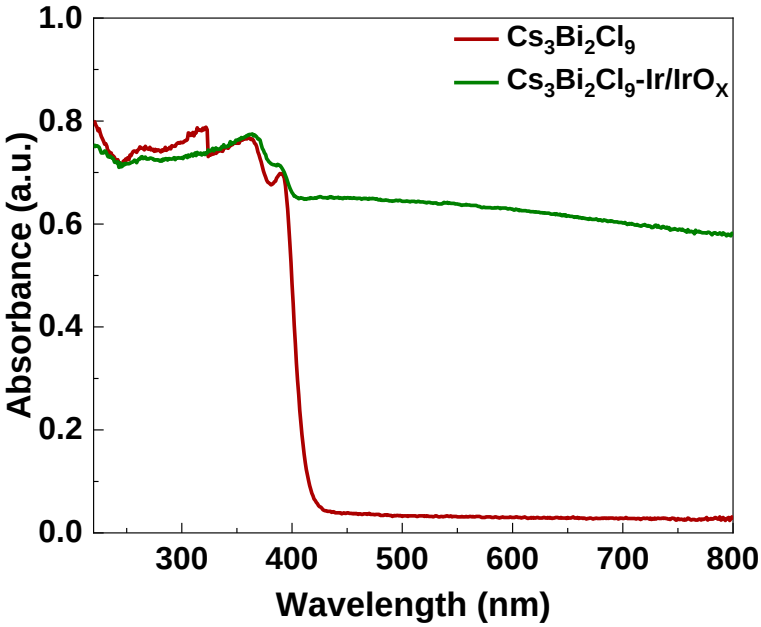

Figure S5. Absolute values of absorbance for $Cs_3Bi_2Cl_9$ and $Cs_3Bi_2Cl_9$-Ir/IrO_X.

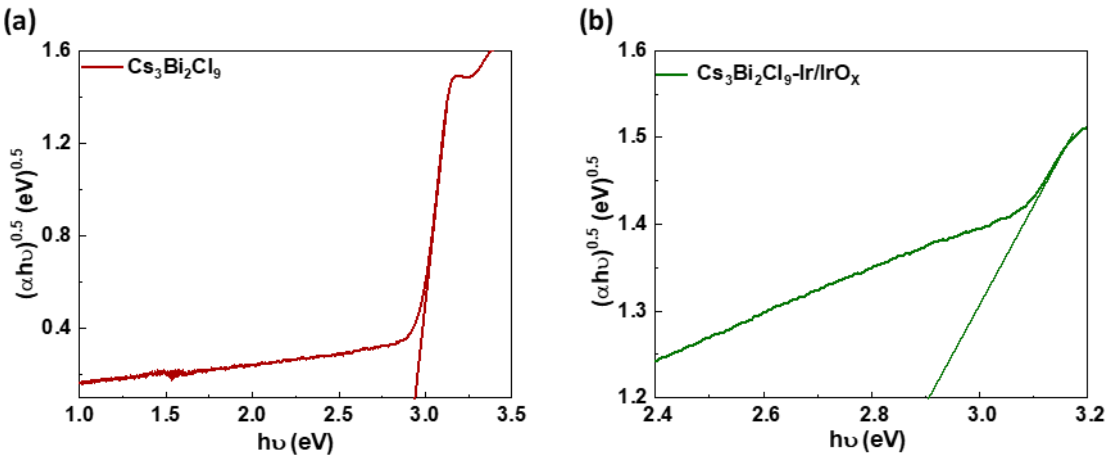

Figure S6. Tauc plot of (a) $Cs_3Bi_2Cl_9$ and (b) $Cs_3Bi_2Cl_9$-Ir/IrO_X.

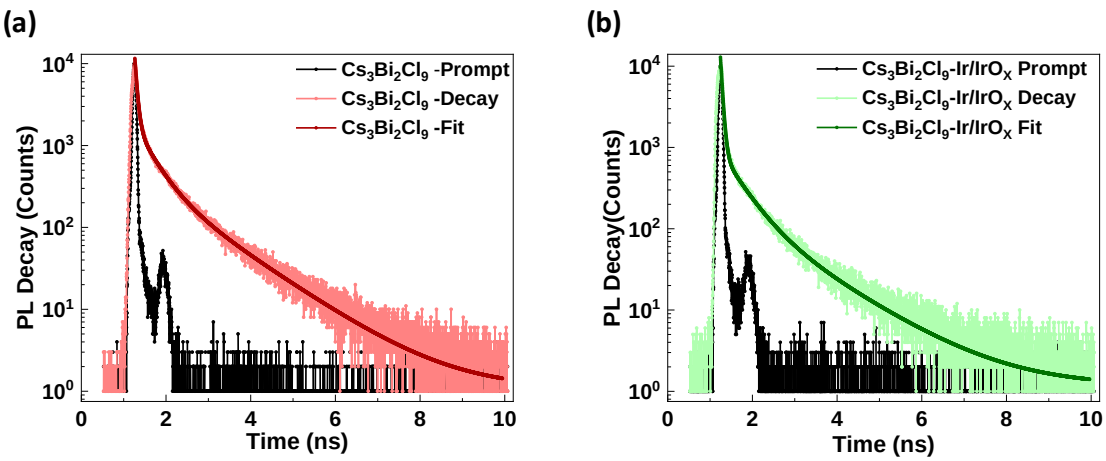

Figure S7. PL decay studies of (a) $Cs_3Bi_2Cl_9$ and (b) $Cs_3Bi_2Cl_9$-Ir/IrO_X.

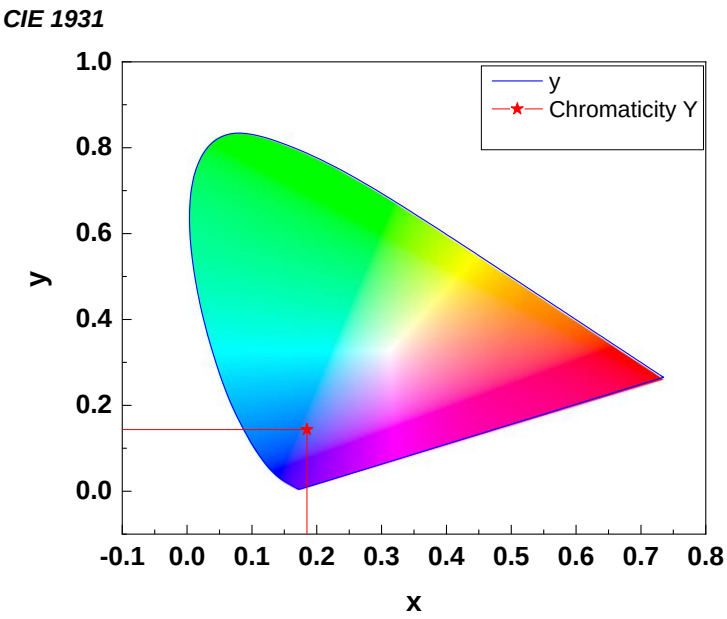

(x, y) = (0.18491, 0.14361)

Figure S8. CIE color coordinates of $Cs_3Bi_2Cl_9$.

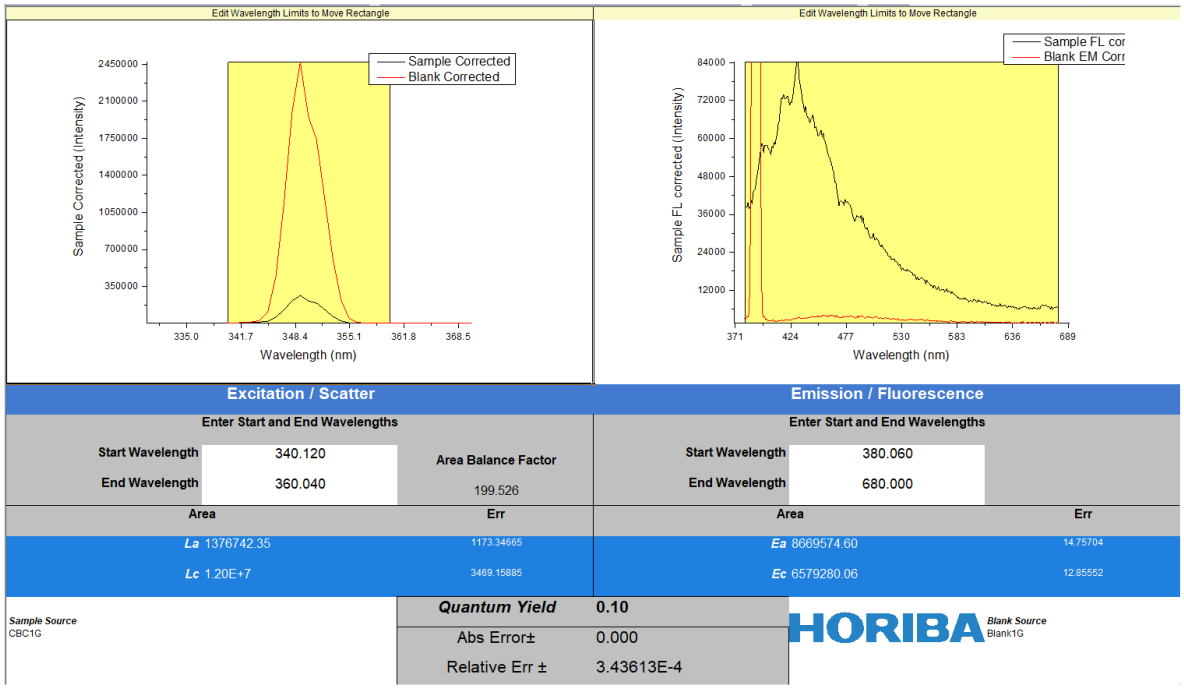

Figure S9. PLQY yield of $Cs_3Bi_2Cl_9$.

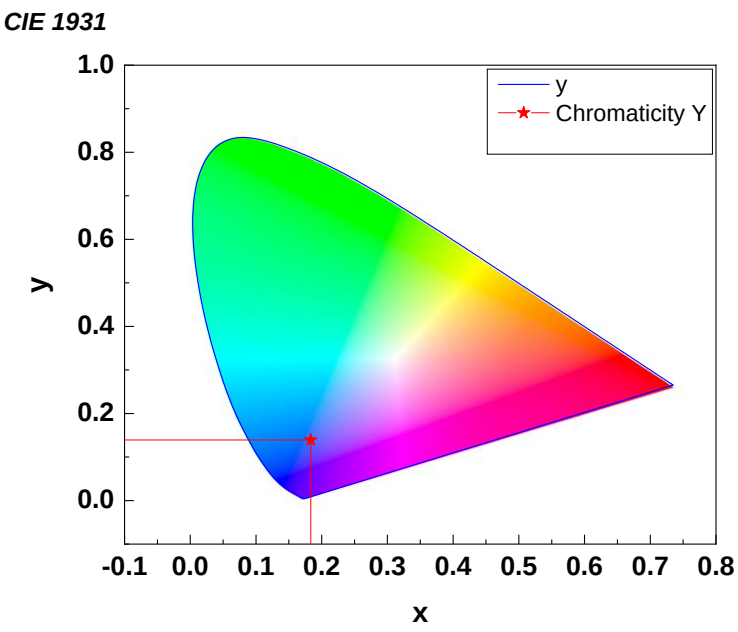

(x, y) = (0.18347, 0.13914)

Figure S10. CIE color coordinates of $Cs_3Bi_2Cl_9$-Ir/IrO_X.

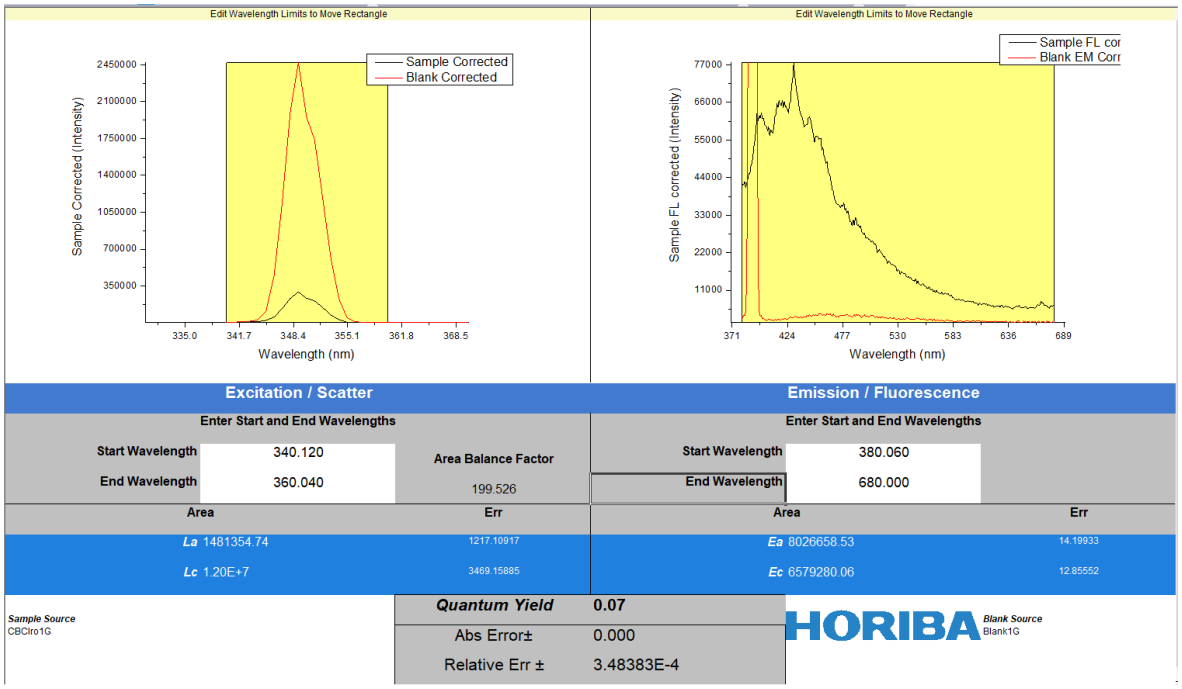

Figure S11. PLQY yield of $Cs_3Bi_2Cl_9$-Ir/IrO_X.

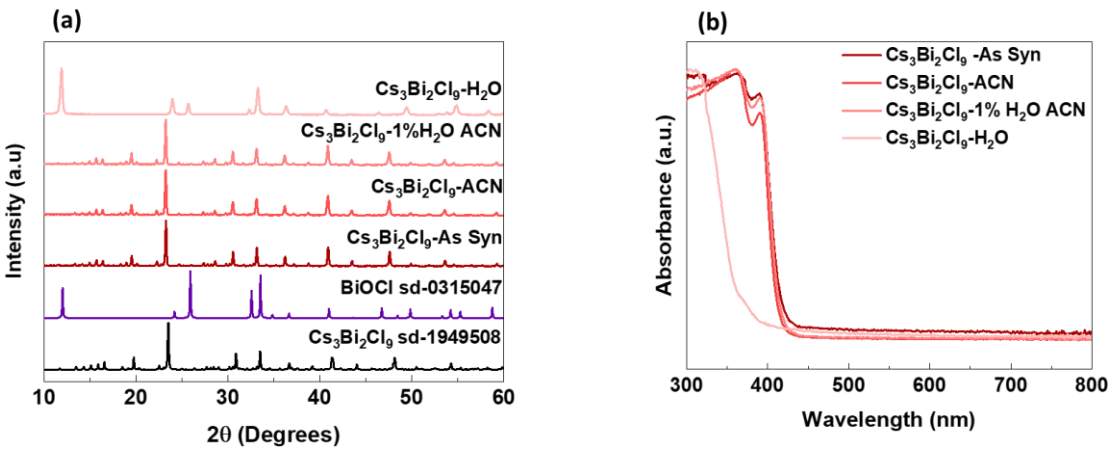

Figure S12. (a) PXRD patterns of $Cs_3Bi_2Cl_9$ in different solvent acetonitrile (ACN) conditions under continuous stirring for 12 hours. (b) corresponding UV-Visible absorption spectra.

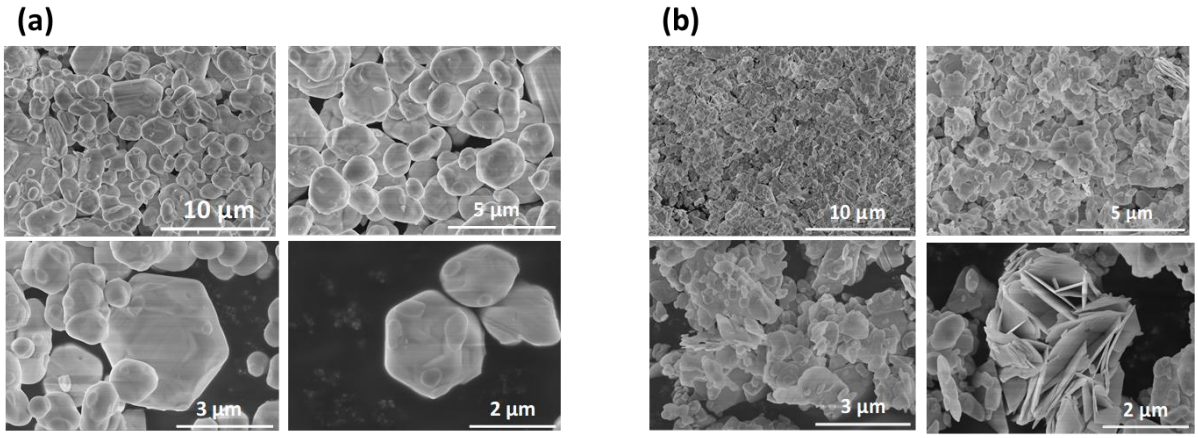

Figure S13. SEM images of (a) $Cs_3Bi_2Cl_9$ in 1 vol% H_2O Acetonitrile (b) pure H_2O.

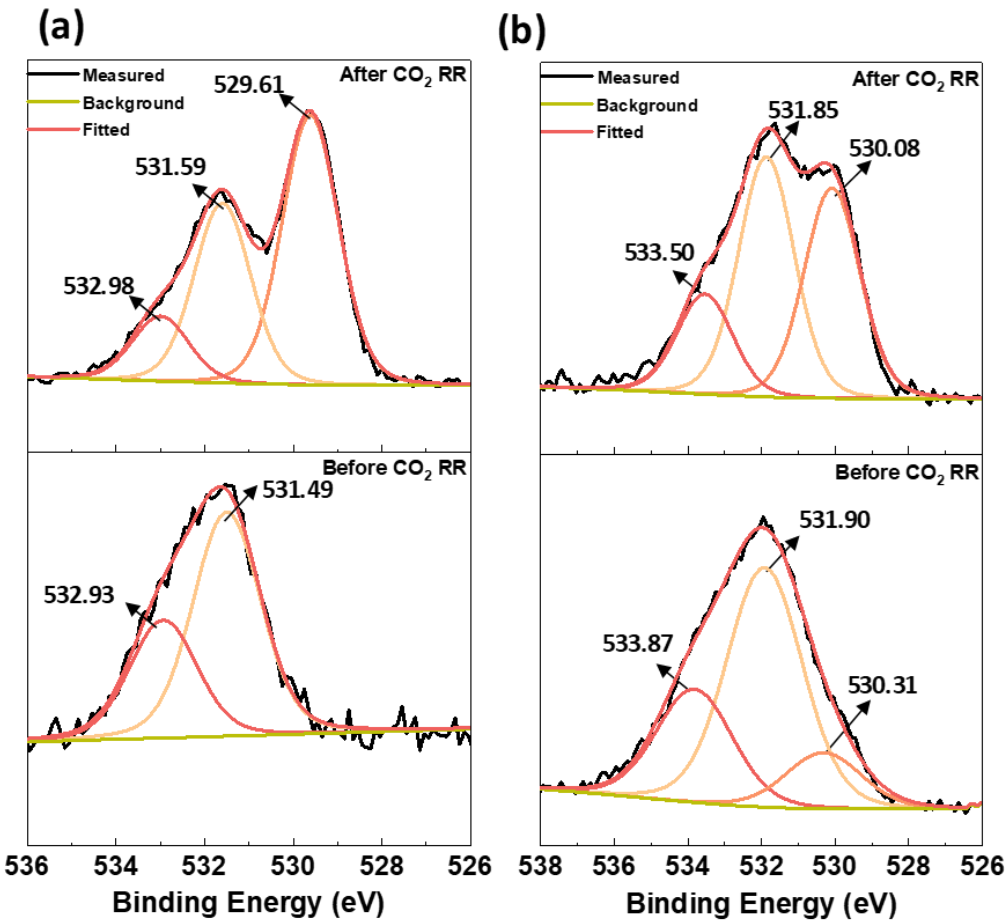

Figure S14. XPS spectra of O 1s (a) $Cs_3Bi_2Cl_9$ (b)$Cs_3Bi_2Cl_9$-Ir/IrO_X before and after CO_2 photoreduction.

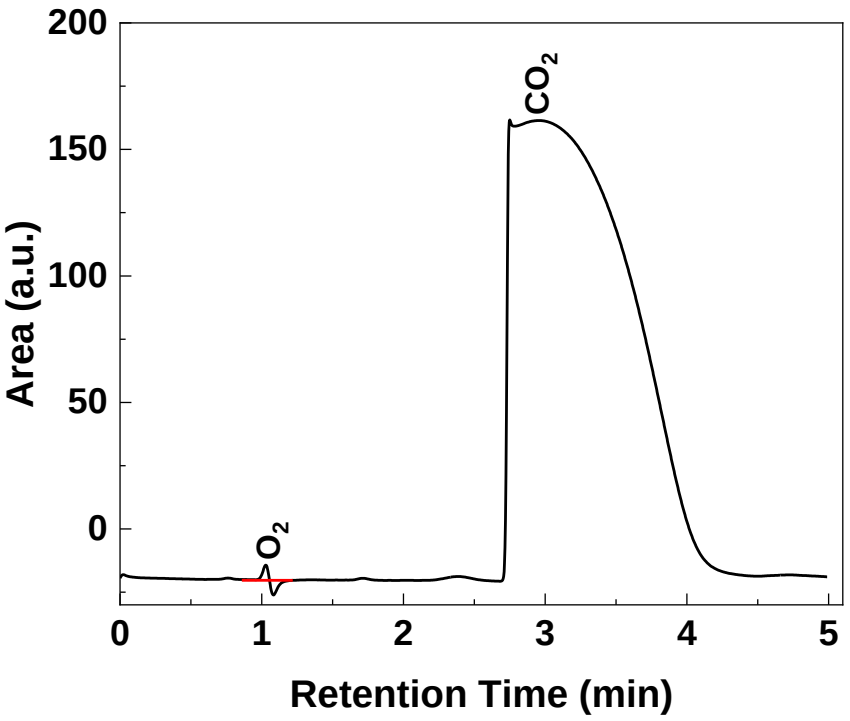

Figure S15. Gas chromatogram of $Cs_3Bi_2Cl_9$-Ir/IrO_X after 5 hours of photocatalytic CO_2 reduction reaction displaying small quantity of oxygen in the head space.

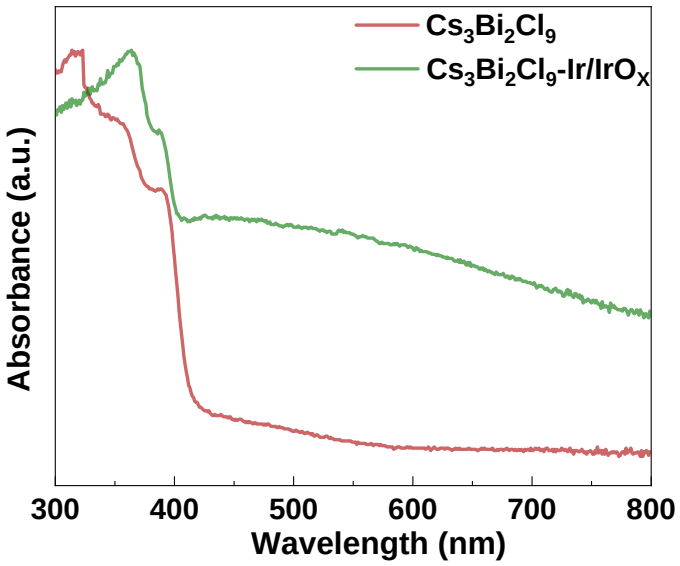

Figure S16. UV-Vis absorption spectra of $Cs_3Bi_2Cl_9$ and $Cs_3Bi_2Cl_9$-Ir/IrO_X after 5 hours of photocatalytic CO_2 reduction reaction.

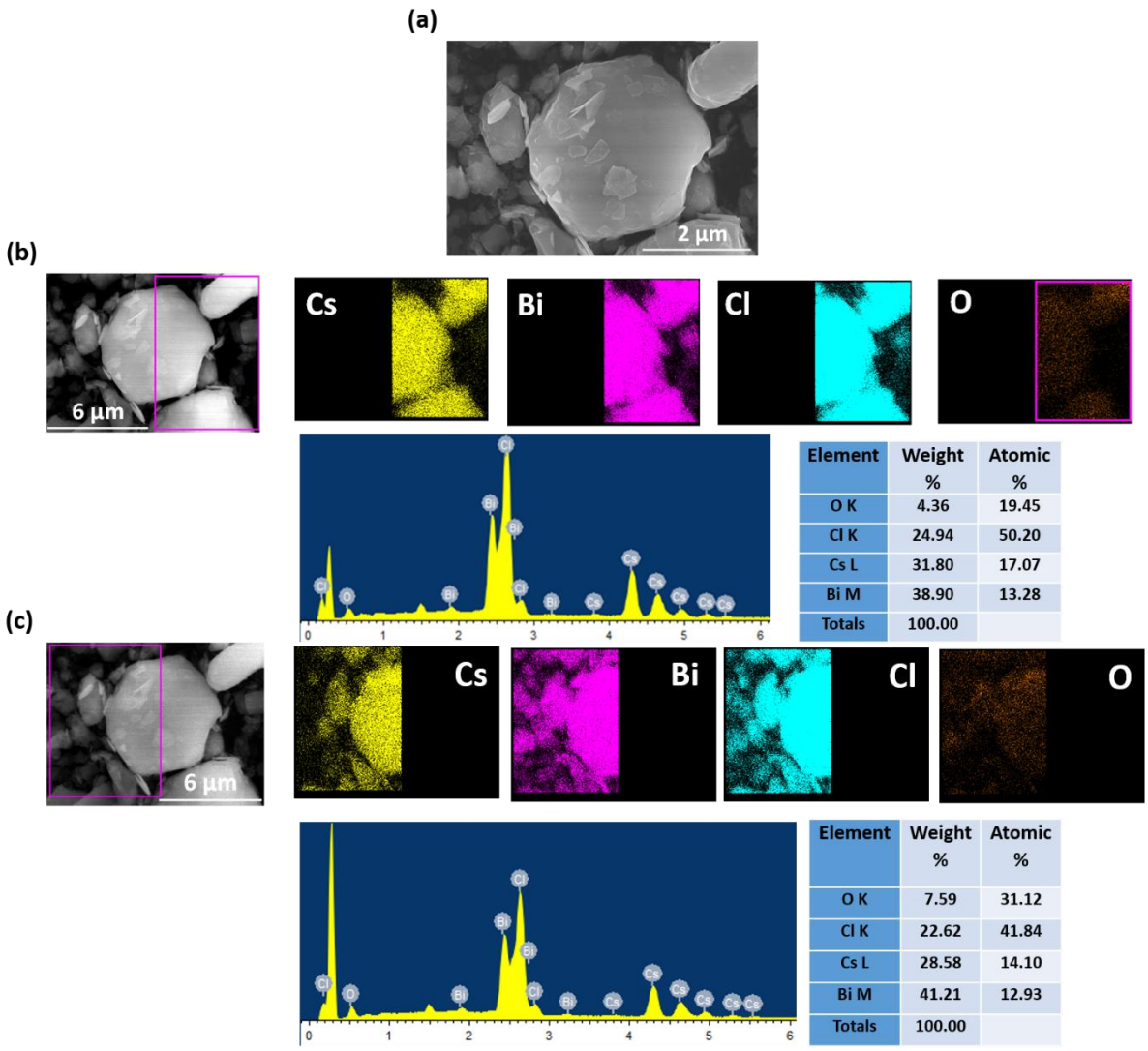

Element	Weight %	Atomic %
O K	4.36	19.45
Cl K	24.94	50.20
Cs L	31.80	17.07
Bi M	38.90	13.28
Totals	100.00	

Element	Weight %	Atomic %
O K	7.59	31.12
Cl K	22.62	41.84
Cs L	28.58	14.10
Bi M	41.21	12.93
Totals	100.00	

Figure S17. (a) SEM image of single $Cs_3Bi_2Cl_9$ particle after 5 hours photocatalytic CO_2 reduction displaying two different morphologies, EDAX mapping in (b) micro particle dominant portion and (c) dominant in the nanosheets portion.

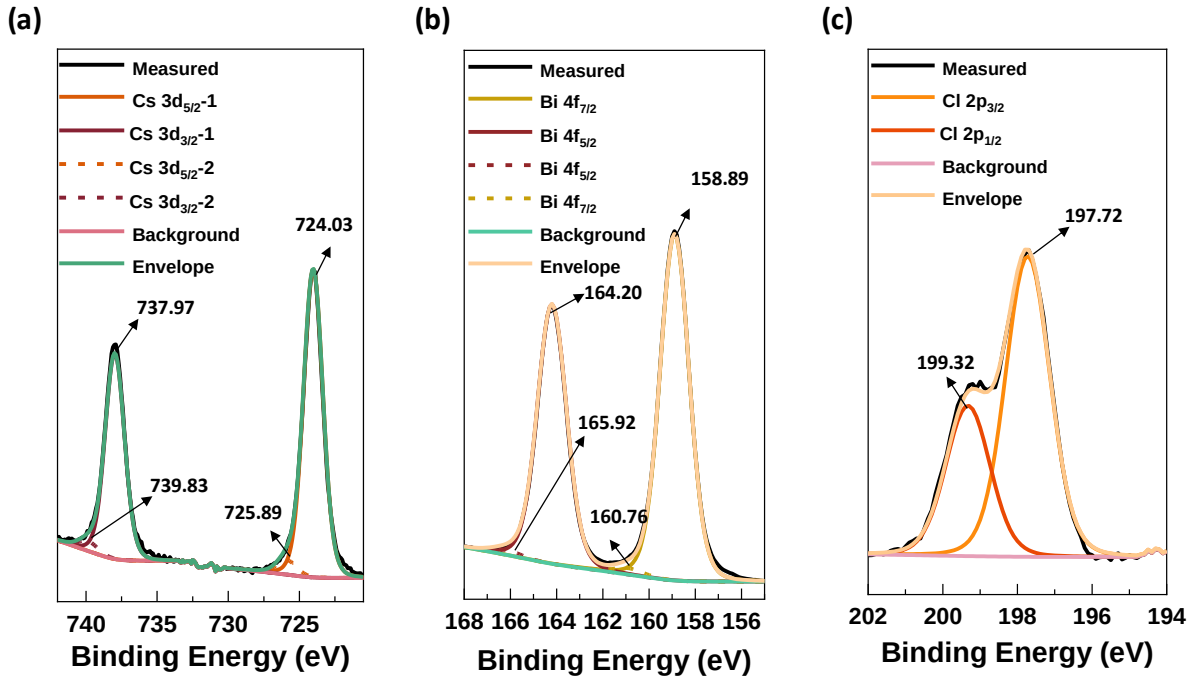

Figure S18. XPS analysis of $Cs_3Bi_2Cl_9$ before and after CO_2 photoreduction: (a) Cs *3d* (b) Bi *4f* (c) Cl *2p*.

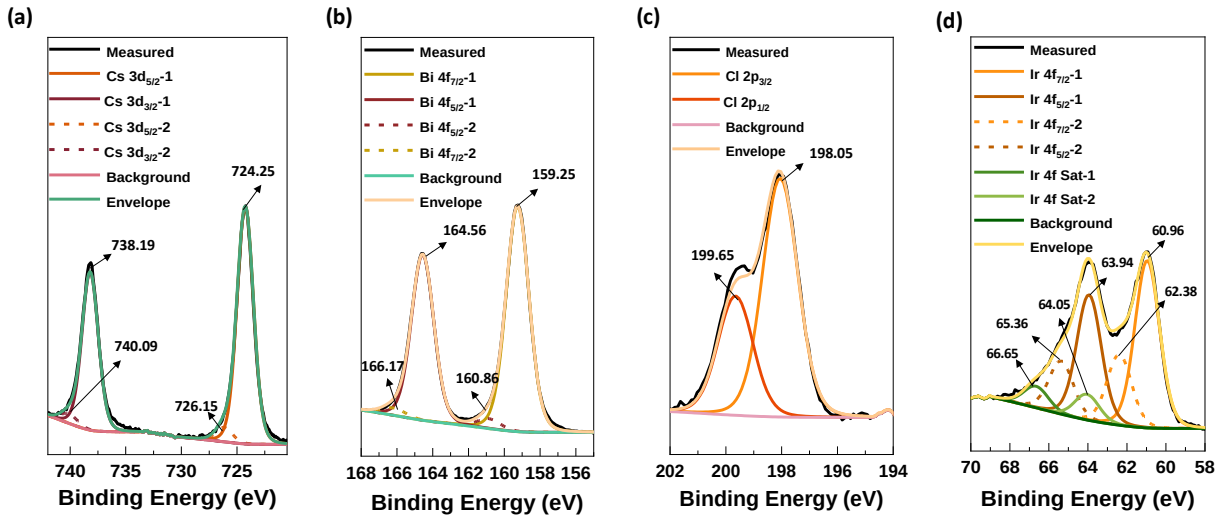

Figure S19. XPS analysis of $Cs_3Bi_2Cl_9$-Ir/IrO_X before and after CO_2 photoreduction: (a) Cs 3d (b) Bi 4f (c) Cl 2p (d) Ir 4f.

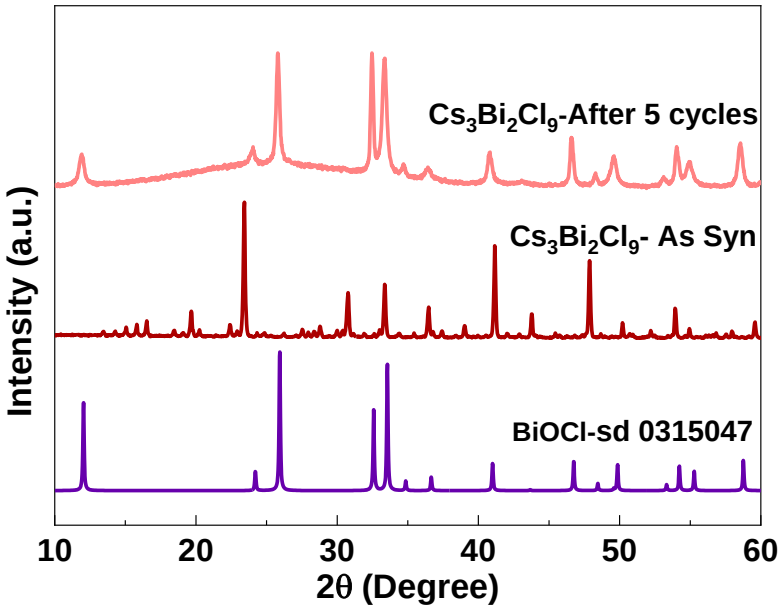

Figure S20. PXRD patterns of $Cs_3Bi_2Cl_9$ after five cycles of photocatalytic CO_2 reduction.

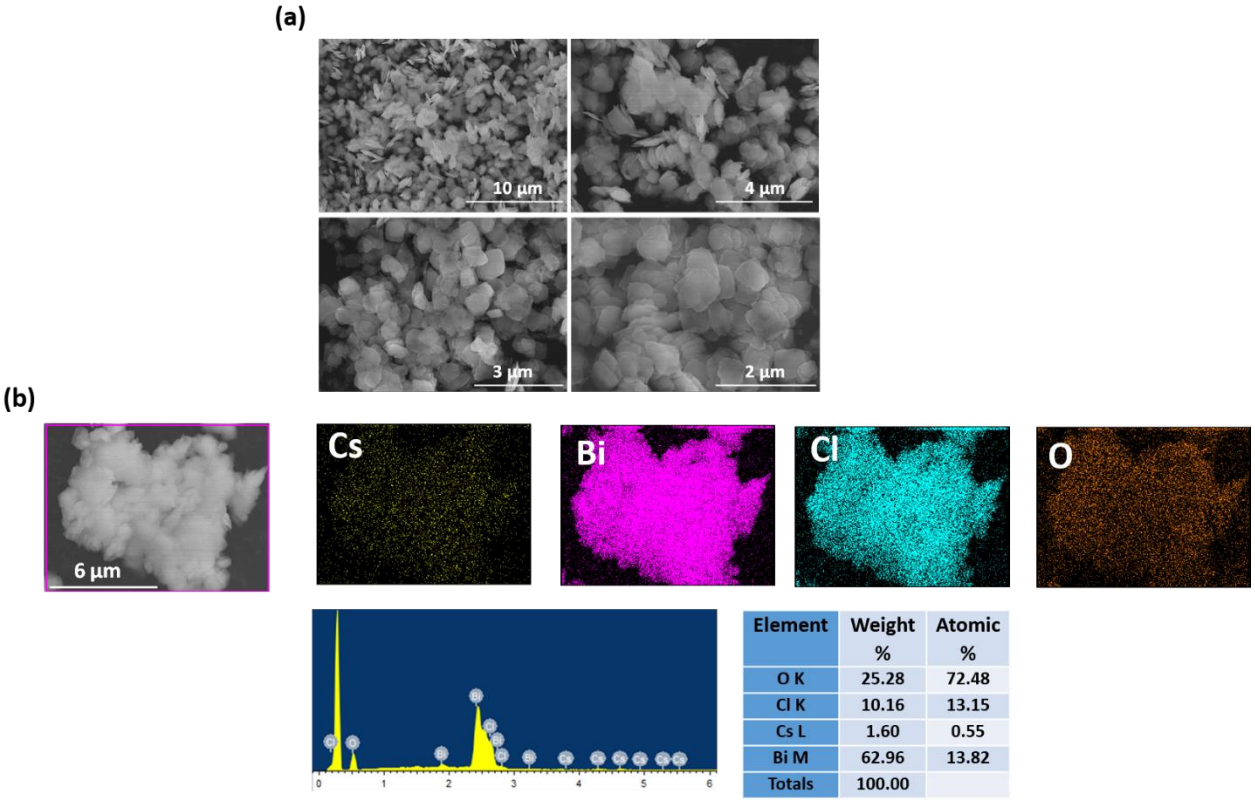

Element	Weight %	Atomic %
O K	25.28	72.48
Cl K	10.16	13.15
Cs L	1.60	0.55
Bi M	62.96	13.82
Totals	100.00	

Figure S21. (a) SEM images of $Cs_3Bi_2Cl_9$ after five cycles of photocatalytic CO_2 reduction **(**b) EDAX elemental mapping.

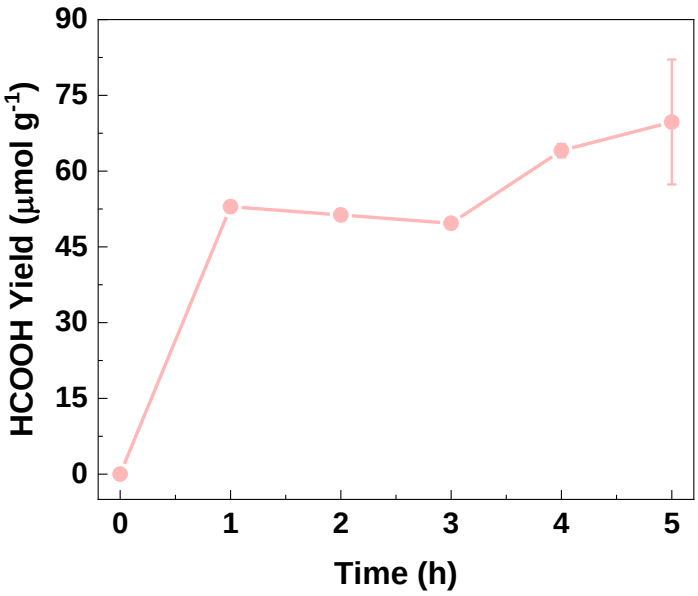

Figure S22. HCOOH yield on $Cs_3Bi_2Cl_9$-H_2O as a function of reaction time

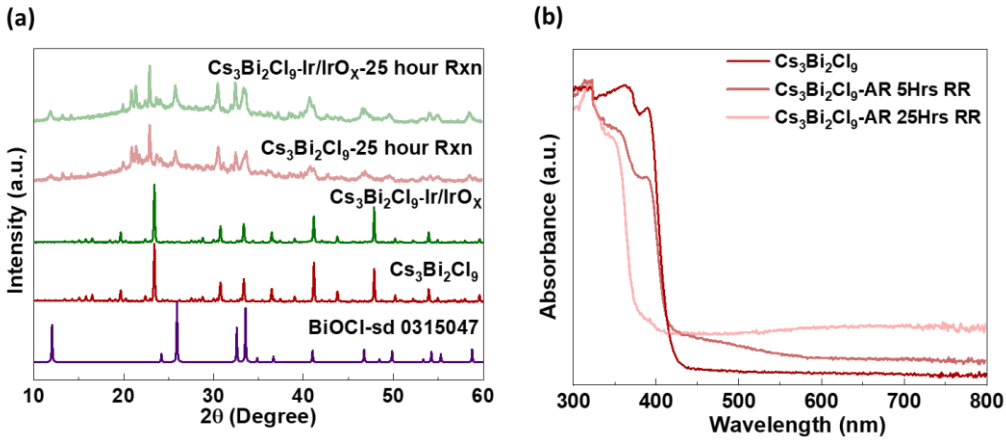

Figure S23. (a) PXRD patterns of $Cs_3Bi_2Cl_9$, $Cs_3Bi_2Cl_9$-Ir/IrO_X after 25 hours of continuous photocatalytic CO_2 reduction and their (b) corresponding absorption spectra.

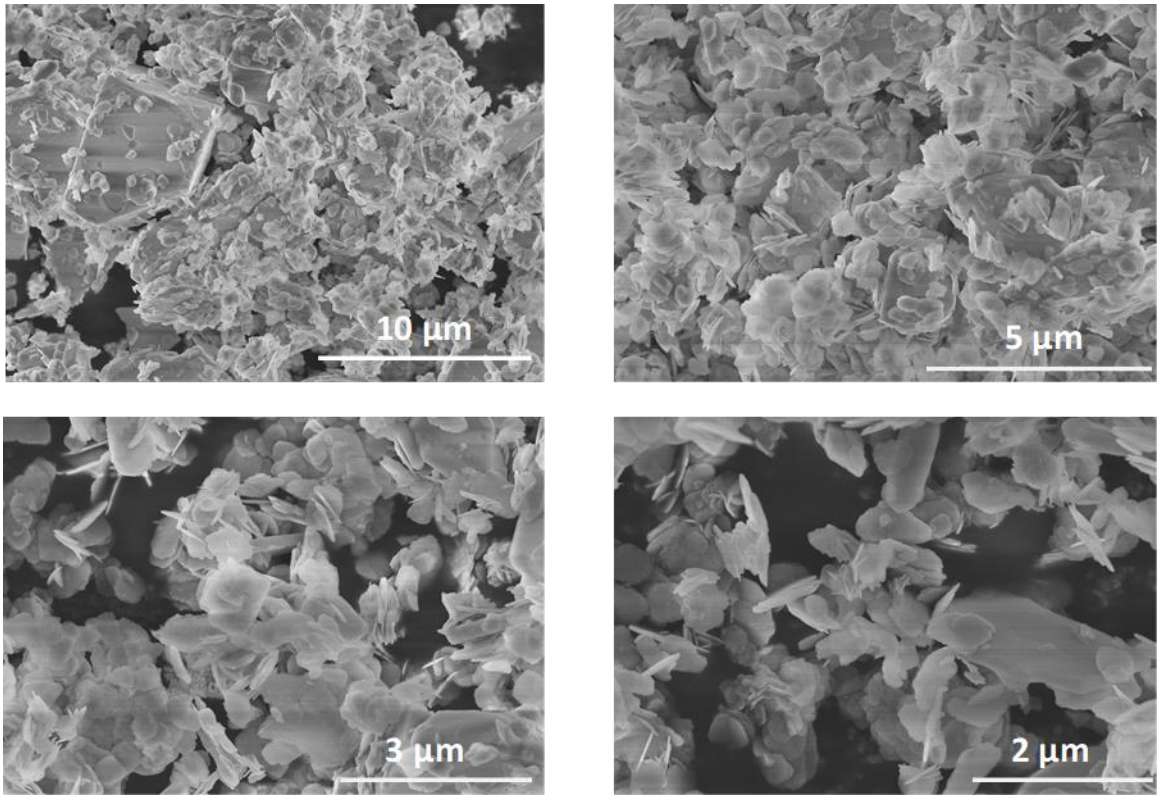

Figure S24. SEM images of $Cs_3Bi_2Cl_9$ after 25 hours continuous photocatalytic CO_2 reduction.

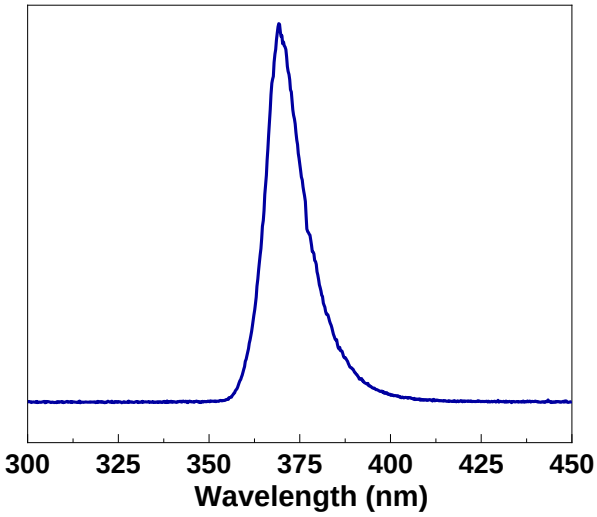

Figure S25. Emission spectrum of 5 W UV-A LED that was used to conduct photocatalytic CO_2 reduction reactions.

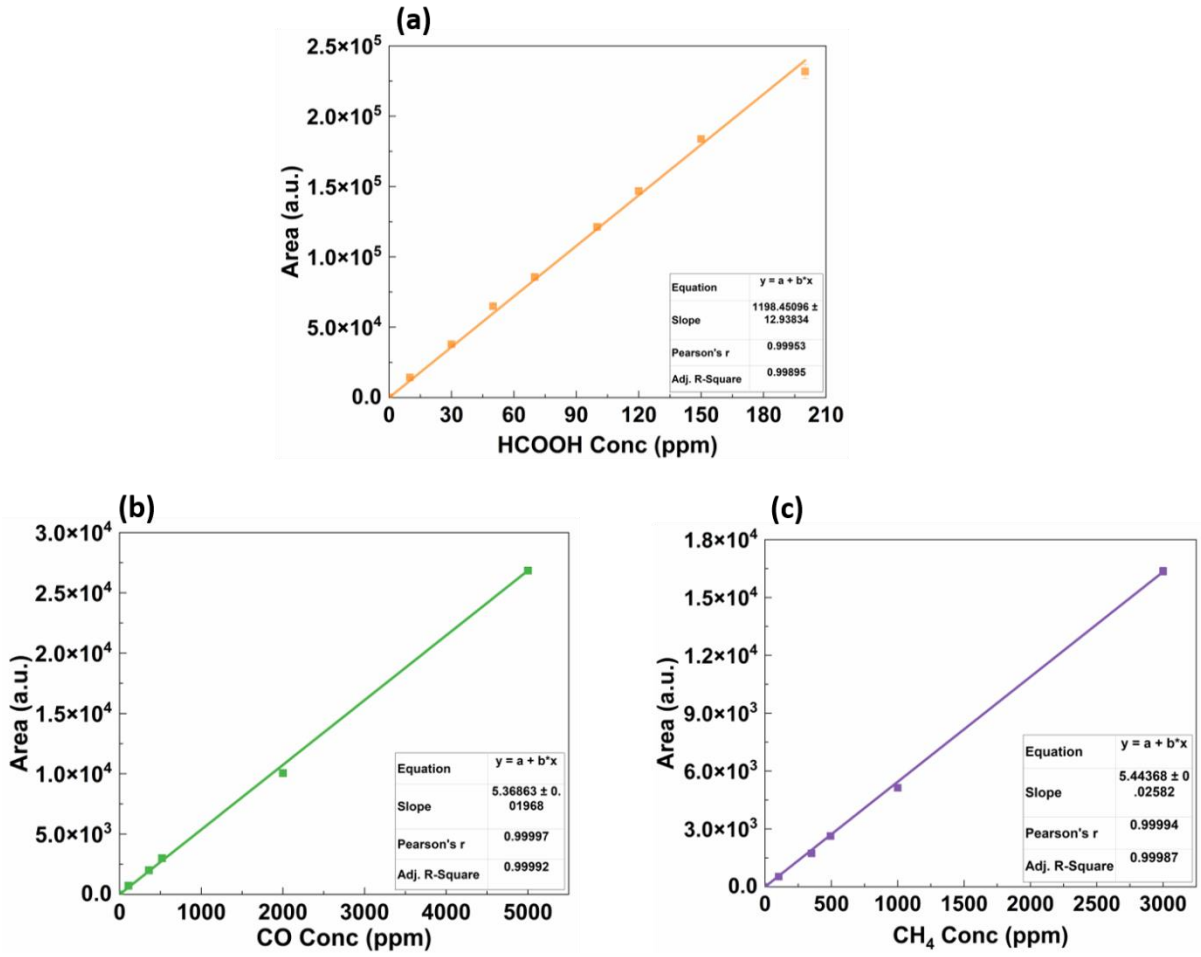

Figure S26. Standardization curves for (a) formic acid (b) carbon monoxide, and (c) methane.

References

1 F. Dong, J. Sheng, Y. He, J. Li, C. Yuan, H. Huang, S. Wang, Y. Sun and Z. Wang, *ACS Nano*, 2020, **14**, 13103–13114.

2 D. Wu, X. Zhao, Y. Huang, J. Lai, J. Yang, C. Tian, P. He, Q. Huang and X. Tang, *J. Phys. Chem. C*, 2021, **125**, 18328–18333.

3 S. S. Bhosale, A. K. Kharade, E. Jokar, A. Fathi, S. M. Chang and E. W. G. Diau, *J. Am. Chem. Soc.*, 2019, **141**, 20434–20442.

4 L. Ding, Y. Ding, F. Bai, G. Chen, S. Zhang, X. Yang, H. Li and X. Wang, *Inorg. Chem.*, , DOI:10.1021/acs.inorgchem.2c04041.

5 Z. L. Liu, R. R. Liu, Y. F. Mu, Y. X. Feng, G. X. Dong, M. Zhang and T. B. Lu, *Sol. RRL*, , DOI:10.1002/solr.202000691.